Acta Med. Okayama, 2020
Vol. 74, No. 2, pp. 129-135

Acta Medica Okayama
http://escholarship.lib.okayama-u.ac.jp/amo/

Original Article

Association between Histological Types and Enhancement of Dynamic CT for Primary Lung Cancer

Shogo Fukuma[a,b*], Takayoshi Shinya[b], Junichi Soh[c,d], Ryuichiro Fukuhara[e], Nanako Ogawa[b], Fumiyo Higaki[f], Takehiro Tanaka[g], Eiki Ichihara[h], Takao Hiraki[b], Shinichi Toyooka[c], and Susumu Kanazawa[b]

Departments of [a]Radiology, [c]General Thoracic Surgery, Breast and Endocrinological Surgery, Okayama University Graduate School of Medicine, Dentistry and Pharmaceutical Sciences, Departments of [b]Radiology, [e]Pediatric Radiology, [g]Pathology, [h]Allergy and Respiratory Medicine, Okayama University Hospital, Okayama 700-8558, Japan, [d]Department of Surgery, Division of Thoracic Surgery, Kindai University Faculty of Medicine, Osaka-Sayama, Osaka 589-8511, Japan, [f]Department of Radiology, Okayama City General Medical Center, Okayama 700-8557, Japan

The aim of this study was to explore enhancement patterns of different types of primary lung cancers on 2-phase dynamic computed tomography (CT). This study included 217 primary lung cancer patients (141 adenocarcinomas [ADs], 48 squamous cell carcinomas [SCCs], 20 small cell lung carcinomas [SCLCs], and 8 others) who were examined using a 2-phase dynamic scan. Regions of interest were identified and mean enhancement values were calculated. After excluding the 20 SCLCs because these lesions had different clinical stages from the other cancer types, the mean attenuation values and subtractions between phases were compared between types of non-small cell lung carcinomas (NSCLCs) using the Kruskal–Wallis test. Late phase attenuation and attenuation of the late minus unenhanced phase (LMU) of SCCs were significantly higher than those of ADs ($p < 0.05$). To differentiate SCC and AD in the late phase, a threshold of 80.21 Hounsfield units (HU) gave 52.9% accuracy. In LMU, a threshold of 52.16 HU gave 59.3% accuracy. Dynamic lung CT has the potential to aid in differentiating among NSCLC types.

Key words: differentiation, dynamic computed tomography, primary lung cancer, enhancement pattern

Lung cancer is the leading cause of cancer death globally [1]. Previous studies have revealed the usefulness of contrast enhanced computed tomography (CT) and dynamic CT for the prediction of tumor benignity of solitary pulmonary nodules (SPN) [2-5]. However, in contrast to the liver [6], kidneys [7], and pancreas [8], no study has focused on differentiating among primary lung cancer types using contrast enhanced dynamic CT. In this study, we explored the enhancement patterns of each type of primary lung cancer using 2-phase lung dynamic CT to clarify the diagnostic capacity of this modality for predicting the pathological types of non-small cell lung carcinomas (NSCLCs). In addition, we assessed the enhancement pattern of small cell lung carcinomas (SCLCs).

Material and Methods

Study populations. This was a single-center retrospective analysis performed using data for 217 patients (128 male, 89 female; age range: 37-92 years)

Received August 6, 2019; accepted November 28, 2019.
*Corresponding author. Phone: +81-86-235-7313; Fax: +81-86-235-7316
E-mail: shogofukuma.pub@gmail.com (S. Fukuma)

Conflict of Interest Disclosures: No potential conflict of interest relevant to this article was reported.

who were seen at our institution from July 2013 to September 2017; the data were taken from a medical database at our institution. Inclusion criteria were as follows: minimum age of 20 years, pathological diagnosis of primary lung cancer untreated before CT scanning, and no treatment prior to diagnosis. Patients diagnosed with other malignancies within 5 years before CT acquisition were excluded. Lesions not described as a nodule using mediastinal window settings (window width: 350 HU [Hounsfield units]; window center: 30 HU) were also excluded. Patients with multiple lesions were included if the lesions were considered histologically homogenous, in which case we measured the largest lesion. All lesions were histologically diagnosed. Our institutional research board approved this retrospective study (approval number: 1809-017) and all patients were given an opportunity to opt out of the study.

CT Examination. All CT examinations were performed using five helical CT scanners: Aquilion Precision (Toshiba Medical Systems, Otawara, Japan; $n=6$), Aquilion One ViSION Edition (Toshiba Medical Systems; $n=148$), Aquilion 64 (Toshiba Medical Systems; $n=10$), SOMATOM Definition Flash (Systems AG, Forchheim, Germany; $n=2$) and Discovery CT750 HD (GE Healthcare, Milwaukee, WI, USA; $n=51$). Images were obtained while patients held their breath using the following parameters: 120 kVp; 300 mA or auto mA mode; section thickness: 5 mm. All studies consisted of 3 scans. After an unenhanced scan, a 2-phase dynamic scan was performed at 30 sec (early phase) and 90 sec (late phase) after intravenous injection of 2.0 ml/kg (maximum of 150 ml) contrast medium.

Image analysis. Two radiologists (S.F. and T.S.) who were not aware of the diagnosis of lung cancer type reviewed the unenhanced and dynamic CT scans. They were instructed to review images using mediastinal window settings and were permitted to adjust the parameters as needed. Maximum tumor diameter was measured using the following lung window conditions: window width: 1,500 HU; window center: −600 HU. Multiplanar reformatting was used to achieve more precise diameter measurements. A round region of interest (ROI) was placed on the most enhanced part of the tumor (mean size ± SD [standard deviation]: 16.51 ± 18.35 mm^2; range: 0.86-258.38 mm^2). Edges of the nodule were avoided to prevent partial volume effects. Vessels, calcifications, and necrotic areas were avoided. The mean enhancement value within the ROI was calculated. For evaluating the uniformity of enhancement timing, round ROIs (mean size ± SD: 311.79 ± 79.62 mm^2; range: 115.68-676.13 mm^2) were placed in the descending aorta at the level of bifurcation of the trachea, and mean HU values in each phase were calculated. Two radiologists were appointed to take these measurements. If they disagreed, the final decision was reached by consensus.

Statistical analysis. Statistical analysis was performed using IBM SPSS Statistics version 22 (IBM, Armonk, NY, USA). Statistical significance was set at $p<0.05$. First, we compared the clinical characteristics of patients using the Kruskal–Wallis test. Second, we compared the mean attenuation values of each type of NSCLC on each phase and subtractions of each phase using the Kruskal–Wallis test. Subtractions consisted of the early phase minus unenhanced phase (EMU), late phase minus unenhanced phase (LMU), and late phase minus early phase (LME). Receiver operating characteristic (ROC) curve analysis was used to determine HU thresholds for suitable sensitivity and specificity to differentiate histological types. The accuracy and area under the curve (AUC) were calculated to evaluate the diagnostic capacity of the determined threshold.

Results

Patients and tumor characteristics. A total of 217 lesions from 217 patients met the inclusion criteria. The histological types were 141 ADs, 48 SCCs, 20 SCLCs, and 8 other carcinomas (4 adenosquamous, 2 large-cell neuroendocrine, 1 large-cell, and 1 spindle-cell tumor). Seven AD patients had multiple pulmonary nodules that were considered homogenous. The mean of the maximum tumor diameter ± SD was 31.1 ± 17.1 mm; range: 7.1-111.1 mm (AD: 29.3 ± 14.6 mm; SCC: 29.6 ± 13.2 mm; SCLC: 46.3 ± 27.8 mm; other: 33.3 ± 27.8 mm). The lesions consisted of 20 partly solid nodules (all AD) and 197 solid nodules. A typical lesion is shown in Fig. 1. The mean number of days ± SD between the CT acquisition and histological sampling or surgery was 17.9 ± 19.1 days (range: −37-152 days).

Enhancement pattern of the tumor and aorta. In the present study, the tumor enhancements of all types showed a progressive enhancement pattern. The mean enhancements of each type are shown in Table 1 and

Fig. 2.

The clinical information of each group is shown in Table 2. Obvious differences were observed in the patient characteristics between SCLC and the other types of lung cancer, especially regarding the clinical stage. For this reason, we considered that it was not appropriate to compare SCLC and the other types of lung cancer. We therefore limited our comparison to the types of non-small cell lung carcinomas (NSCLCs), and analyzed the enhancement pattern of SCLC independently.

The mean aortic attenuation value of SCLC was 302.6 HU, and that of NSCLC was 320.1 HU in the early phase ($p = 0.088$). In the late phase, the mean aortic attenuation value of SCLC was 140.8 HU and that of NSCLC was 150.5 HU ($p = 0.051$). The weights of

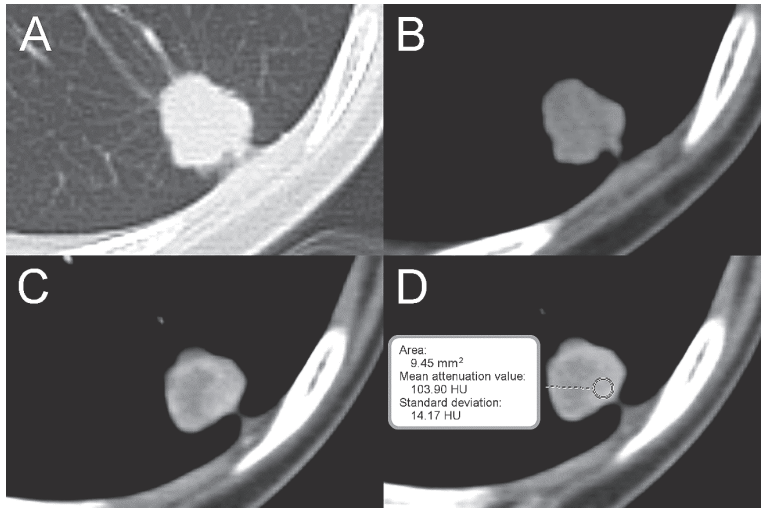

Fig. 1 A 67-year-old woman with primary lung adenosquamous carcinoma in the left lower lobe. (**A**) A lobulated and speculated nodule with a maximum diameter of 17.2 mm. The maximum average Hounsfield unit (HU) measurements were 51.0 HU in the unenhanced phase (**B**), 112.5 HU in the early phase (**C**), and 103.9 HU in the late phase (**D**). Thirty-three days after this scan, a left lower lobectomy was performed along with pathological diagnosis.

Table 1 The mean attenuation values of types, of total lesions, and of non-small cell lung carcinoma (NSCLC)

	AD (HU)*	SCC (HU)*	SCLC (HU)*	Other (HU)*	NSCLC (HU)*	Total (HU)*
Unenhanced	30.95 (± 12.04)	33.94 (± 11.67)	37.31 (± 10.57)	35.97 (± 11.90)	31.88 (± 11.99)	32.38 (± 11.94)
Early	70.44 (± 23.32)	75.40 (± 15.52)	64.87 (± 13.17)	82.86 (± 21.74)	72.16 (± 21.74)	71.48 (± 21.18)
Late	80.95 (± 20.92)	92.01 (± 15.29)	68.55 (± 20.61)	90.00 (± 20.90)	84.01 (± 20.21)	82.59 (± 20.69)
Early — unenhanced	39.49 (± 20.41)	41.46 (± 17.52)	27.56 (± 11.45)	46.89 (± 16.21)	40.27 (± 19.57)	39.10 (± 19.30)
Late — unenhanced	50.00 (± 16.52)	58.07 (± 16.65)	31.24 (± 17.99)	54.04 (± 20.13)	52.13 (± 16.97)	50.20 (± 18.06)
Late — early	10.51 (± 18.13)	16.61 (± 13.65)	3.69 (± 18.46)	7.15 (± 24.35)	11.86 (± 17.56)	11.10 (± 17.76)

HU, Hounsfield unit; AD, adenocarcinoma; SCC, squamous cell carcinoma; SCLC, small cell lung carcinoma; NSCLC, non-small cell lung carcinoma.

*Data is expressed as mean ± standard deviation.

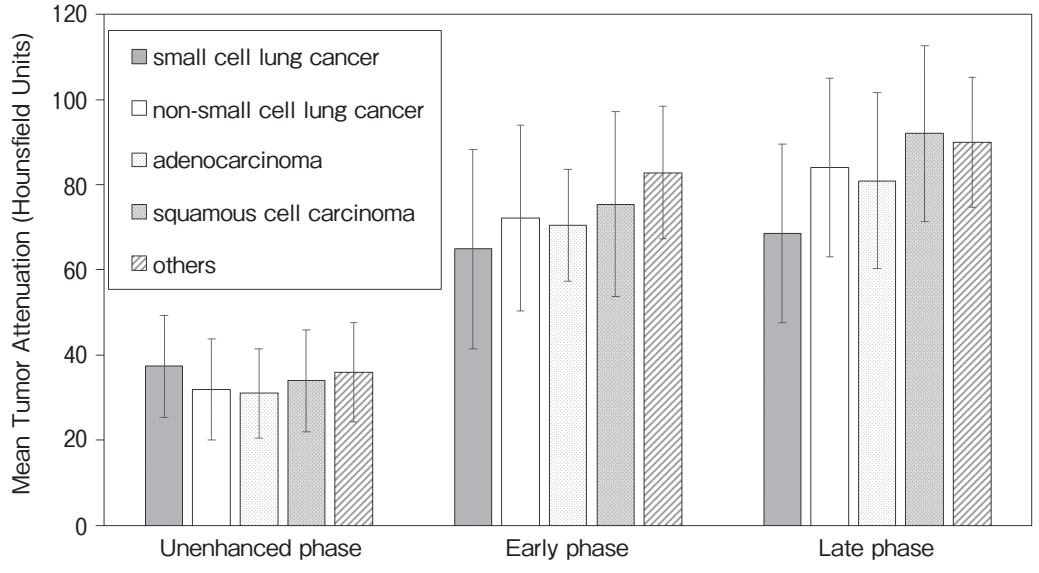

Fig. 2 Mean attenuation value of tumors in each phase of each type. Error bars show the standard deviation.

Table 2 Clinical information of patients with each histological type

	AD (n = 141)	SCC (n = 48)	SCLC (N = 20)	Others (n = 8)
Sex (*n*)				
Male/Female	68/73	42/6	13/7	5/3
Age (y)				
Median/range	69/42–92	72.5/37–91	68/54–82	66/44–78
Smoking history (*n*)				
Past or current/Never	81/60	45/3	19/1	7/1
Final diagnostic method (*n*)				
Surgical resection	140	48	3	7
Percutaneous biopsy	0	0	3	0
Bronchoscopy	1	0	14	1
Patients with multiple lesions (*n*)	7	0	0	0
Maximum tumor diameter (mm)*	29.3 (± 14.6)	29.6 (± 13.2)	46.3 (± 27.8)	33.3 (± 27.8)
Clinical stage				
I	95	32	3	4
II	35	9	2	1
III	10	7	6	2
IV	1	0	9	1

The breakdown of patients by clinical stage was based on the eighth edition of the "TNM classification of malignant tumors" published by the Union for International Cancer Control, which is widely used for classification.
AD, adenocarcinoma; SCC, squamous cell carcinoma; SCLC, small cell lung carcinoma; SD, standard deviation.
*Data expressed as mean ± standard deviation.

patients at CT acquisition ± SD were 59.18 ± 11.01 kg in the NSCLC group, and 62.28 ± 14.40 kg in the SCLC group ($p = 0.536$, Mann–Whitney U test).

Adenocarcinoma vs. squamous cell carcinoma. Kruskal–Wallis analysis revealed there was no significant difference in age and maximum tumor diameter among the different types of NSCLC ($p = 0.064$, 0.758, respectively). Only sex was significantly different among NSCLC types ($p < 0.001$), with the percentage of females being significantly higher in the AD than the SCC group according to the Dunn–Bonferroni post hoc analysis ($p < 0.001$). Attenuation of SCC was significantly higher than that of AD in the late phase and LMU ($p < 0.05$) (Table 3). Attenuation thresholds and AUC were calculated by ROC analysis (Table 4 and Fig. 3). For the late phase, a threshold of 80.21 HU gave 79.2% sensitivity, 44.0% specificity, and 52.9% accuracy. For the LMU, a threshold of 52.16 HU gave 60.4% sensitivity, 58.9% specificity, and 59.3% accuracy. A combination of both criteria gave 56.3% sensitivity, 63.8% specificity, and 61.9% accuracy. Mean attenuation values of the aorta between AD and SCC were not significantly different in either the early phase or late phase (Kruskal–Wallis test, $p = 0.301$ and 0.927, respectively).

Discussion

Contrast enhanced CT [2] and dynamic CT [3-5] are useful for predicting tumor benignity of SPNs. However, few studies have used CT to differentiate among lung cancer types. While non-contrast enhanced CT [9-11] and contrast enhanced CT [12] have been used to differentiate lung cancer types, no studies have assessed the diagnostic capacity of dynamic CT.

We found that the enhancement patterns of each type were progressive. A study by Jeong *et al.* [3] categorized the enhancement patterns of 107 SPNs from 30 sec to 15 min and found that AD ($n = 33$), SCC ($n = 3$), and SCLC ($n = 1$) all showed wash-in and wash-out patterns. In their study, the time-to-peak enhancement of malignant nodules was 3.2 ± 2.7 min. The progressive enhancement patterns within 90 sec observed in our study may reflect this "wash-in" phase. The difference between the peak- and pre-enhancement value of malignant nodules reported by Jeong *et al.* was 50 ± 16.7 HU [3], similar to our LMU result of 50.20 ± 18.06 HU.

Table 3 Statistical comparisons of the mean attenuation values of adenocarcinoma (AD), squamous cell carcinoma (SCC), and other cancer types in each phase using the Kruskal–Wallis test and post hoc Dunn–Bonferroni test

	Kruskal–Wallis test significance	Post-hoc analysis significance		
		AD vs SCC	AD vs Other	SCC vs Other
Unenhanced	0.256			
Early	0.056			
Late	0.004*	0.003*	1.000	1.000
Early — Unenhanced	0.370			
Late — Unenhanced	0.037*	0.031*	1.000	1.000
Late — Early	0.017*	0.051	0.621	0.074

AD, adenocarcinoma; SCC, squamous cell carcinoma; HU, Hounsfield unit; vs, versus.
*$p < 0.05$.

Table 4 ROC Analysis of the diagnostic capacity for differentiating squamous cell carcinoma (SCC) from adenocarcinoma (AD)

	Attenuation threshold value (HU)	Sensitivity (%)	Specificity (%)	PPV (%)	NPV (%)	Accuracy (%)	AUC
Differentiation of SCC from AD							
Late	80.21	79.2	44.0	32.5	86.1	52.9	0.661
Late — unenhanced	52.16	60.4	58.9	33.3	81.4	59.3	0.625

SCC, squamous cell carcinoma; AD, adenocarcinoma; HU, Hounsfield unit; PPV, positive predictive value; NPV, negative predictive value; AUC, area under the curve.

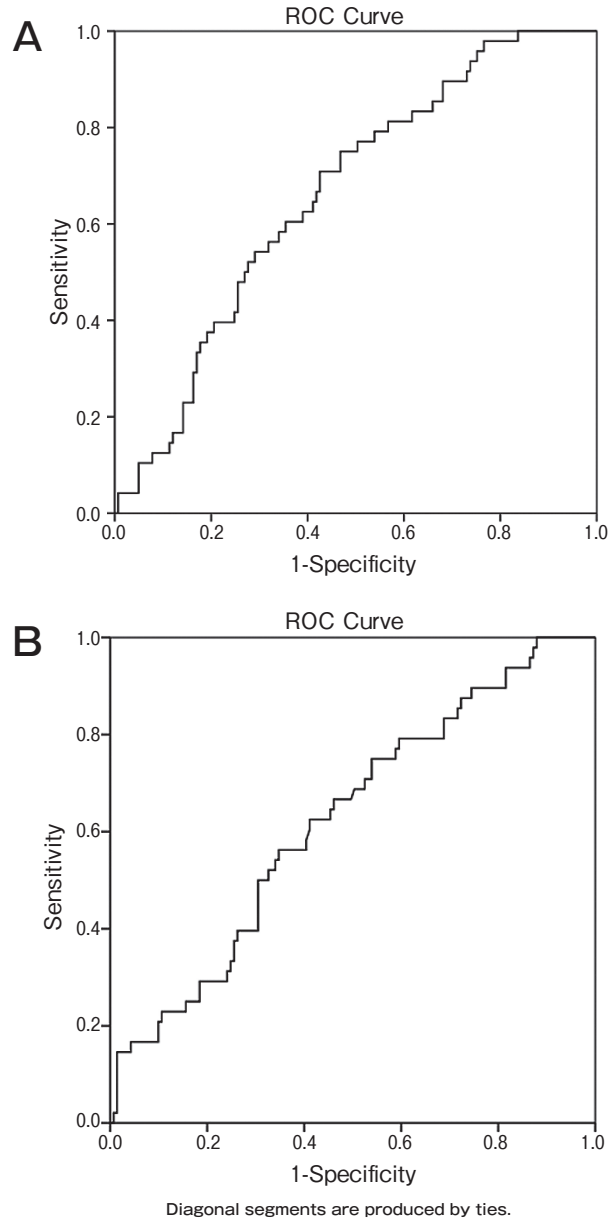

Fig. 3 ROC curve for discriminating adenocarcinoma from squamous cell carcinoma in the late phase (A) and subtraction of the late and unenhanced phase (B).

We also found that the enhancement of SCC was higher than that of AD in the late phase and LMU. Thresholds of 80.21 HU in the late phase and 52.16 HU in LMU resulted in AUCs of 0.661 and 0.625, respectively. Combining the 2 parameters increased the accuracy to 61.9%. For comparison, E L *et al.* [10] and Zhu *et al.* [11] used a radiomics approach and reported AUCs of 0.655 and 0.893 for samples of 88 AD/93 SCC, and 53 AD/76 SCC, respectively. Ferreira Junior *et al.* [12] reported an AUC of 0.81 using a radiomics approach to contrast enhanced CT for 30 AD and 15 SCC. These differences could have arisen from the different numbers of patients, training datasets, or methods of feature selection. Although the AUC using our dynamic CT method was lower than the AUCs for these prior studies, our method was significantly effective for differentiating between AD and SCC. Future research should combine dynamic CT and radiomics to improve the diagnostic capacities.

Finally, SCLCs showed relatively low attenuation values when compared with NSCLCs in this study. However, the clinical stage of SCLCs was higher than that of the other types in our cohort, which made it difficult to compare SCLCs with the other types in this study. Additional studies of larger cohorts under a uniform clinical background might reveal the true clinical impact of the enhancement of SCLCs in dynamic CT. Further, the aortic enhancement of SCLCs did not differ significantly from that of NSCLCs; however, the former enhancement did have a lower value, which may have affected the enhancement of SCLCs. There are some other factors which may partly explain the lower aortic enhancement of SCLCs. First, our patients with SCLCs tended to be heavier than our patients with NSCLCs, although the difference was not statistically significant. Second, a previous study reported that a flow rate of 2 mL/sec was associated with insufficient contrast enhancement of the pulmonary artery, whereas the enhancement at a flow rate of 3 mL/sec was associated with lower frequency of insufficient contrast enhancement [13]. In this study, we used a flow rate of 2 mL/sec, which might have led to the insufficient contrast enhancements in this study.

Our retrospective study had several limitations that could have influenced the results. First, we did not match the clinical characteristics of patients between cancer types. The SCLCs showed a higher clinical stage in our cohort, which made it difficult to compare them with the other cancer types in this study. In addition, the AD group had a significantly higher ratio of females than the SCC group. Second, there were variations in the CT equipment used to collect the data. Third, the section thickness of 5 mm may have been too thick to evaluate lung nodules. However, we tried to avoid the partial volume effect as much as possible. Fourth, we

did not investigate the pathological backgrounds, although they could have contributed to the difference of enhancement patterns among types. Previous studies indicated a relationship between the enhancement of lung tumors and their histological characteristics, such as microvessel density, vascular endothelial growth factor (VEGF) staining [14], and tumor fibrosis [15]. However, the histological factors that can explain the differences in enhancement between tumor types are still unknown, so further studies on radiological-pathological correlations, such as those discussed above, will be needed to clarify this matter. Finally, we did not explore the diagnostic capacity of dynamic lung CT for the other types of lung cancer.

In conclusion, dynamic lung CT has the potential to aid in differentiating among primary lung cancer types, especially by using the late phase.

References

1. Dela Cruz CS, Tanoue LT and Matthay RA: Lung cancer: epidemiology, etiology, and prevention. Clin Chest Med (2011) 32: 605–644.
2. Swensen SJ, Viggiano RW, Midthun DE, Müller NL, Sherrick A, Yamashita K, Naidich DP, Patz EF, Hartman TE, Muhm JR and Weaver AL: Lung nodule enhancement at CT: multicenter study. Radiology (2000) 214: 73–80.
3. Jeong YJ, Lee KS, Jeong SY, Chung MJ, Shim SS, Kim H, Kwon OJ and Kim S: Solitary pulmonary nodule: characterization with combined wash-in and washout features at dynamic multi-detector row CT. Radiology (2005) 237: 675–683.
4. Khanduri S, Bhagat S, Shokeen P, Kumar G, Khanduri S and Singh B: Rationale of Using Dynamic Imaging for Characterization of Suspicious Lung Masses into Benign or Malignant on Contrast Enhanced Multi Detector Computed Tomography. J Clin Imaging Sci (2017) 7: 24.
5. Ye XD, Ye JD, Yuan Z, Li WT and Xiao XS: Dynamic CT of solitary pulmonary nodules: comparison of contrast medium distribution characteristic of malignant and benign lesions. Clin Transl Oncol (2014) 16: 49–56.
6. Ariff B, Lloyd CR, Khan S, Shariff M, Thillainayagam AV, Bansi DS, Khan SA, Taylor-Robinson SD and Lim AK: Imaging of liver cancer. World J Gastroenterol (2009) 15: 1289–1300.
7. Kim JK, Kim TK, Ahn HJ, Kim CS, Kim KR and Cho KS: Differentiation of subtypes of renal cell carcinoma on helical CT scans. AJR Am J Roentgenol (2002) 178: 1499–1506.
8. Low G, Panu A, Millo N and Leen E: Multimodality imaging of neoplastic and nonneoplastic solid lesions of the pancreas. Radiographics (2011) 31: 993–1015.
9. Jiang B, Takashima S, Miyake C, Hakucho T, Takahashi Y, Morimoto D, Numasaki H, Nakanishi K, Tomita Y and Higashiyama M: Thin-section CT findings in peripheral lung cancer of 3 cm or smaller: are there any characteristic features for predicting tumor histology or do they depend only on tumor size? Acta Radiol (2014) 55: 302–308.
10. E L, Lu L, Li L, Yang H, Schwartz LH and Zhao B: Radiomics for Classification of Lung Cancer Histological Subtypes Based on Nonenhanced Computed Tomography. Acad Radiol (2019) 26: 1245–1252.
11. Zhu X, Dong D, Chen Z, Fang M, Zhang L, Song J, Yu D, Zang Y, Liu Z, Shi J and Tian J: Radiomic signature as a diagnostic factor for histologic subtype classification of non-small cell lung cancer. Eur Radiol (2018) 28: 2772–2778.
12. Ferreira Junior JR, Koenigkam-Santos M, Cipriano FEG, Fabro AT and Azevedo-Marques PM: Radiomics-based features for pattern recognition of lung cancer histopathology and metastases. Comput Methods Programs Biomed (2018) 159: 23–30.
13. Ozawa Y, Hara M and Shibamoto Y: The frequency of insufficient contrast enhancement of the pulmonary artery in routine contrast-enhanced chest CT and its improvement with an increased injection rate: a prospective study. J Thorac Imaging (2011) 26: 42–47.
14. Yi CA, Lee KS, Kim EA, Han J, Kim H, Kwon OJ, Jeong YJ and Kim S: Solitary pulmonary nodules: dynamic enhanced multi-detector row CT study and comparison with vascular endothelial growth factor and microvessel density. Radiology (2004) 233: 191–199.
15. Iwano S, Koike W, Matsuo K, Okada T, Shimoyama Y and Naganawa S: Correlation between dual-phase dynamic multi-detector CT findings and fibrosis within lung adenocarcinoma tumors. Eur J Radiol (2011) 80: e470–475.